

# Adsorption of a Polyelectrolyte Chain on a Charged Surface: A Monte Carlo Simulation of Scaling Behavior

V. Yamakov<sup>1,3</sup>, A. Milchev<sup>1</sup>, O. Borisov<sup>2</sup> and B. Dünweg<sup>3</sup>

<sup>1</sup> *Institute for Physical Chemistry, Bulgarian Academy of Sciences, G. Bonchev Street, Block 11, 1113 Sofia, Bulgaria*

<sup>2</sup> *BASF AG, ZX/ZC, D-67056 Ludwigshafen, Germany*

<sup>3</sup> *Max-Planck-Institut für Polymerforschung, Ackermannweg 10, D-55128 Mainz, Germany*

We study the adsorption of a charged polymer chain (polyelectrolyte) grafted to an oppositely charged surface by means of an off-lattice Monte Carlo simulation. We consider the effects of chain ionization, surface charge density, and solution ionic strength on the conformational and interfacial properties of the model system. By varying the chain length of the polyelectrolyte over a broad range we determine the critical parameters for adsorption and find a very good agreement with recent scaling predictions for polyelectrolyte adsorption in the various regimes of chain ionization and salt content of the solution.

## 1. Introduction

Polyelectrolyte adsorption on charged surfaces is nowadays broadly used in industrial applications. Many colloidal suspensions, for instance, can be stabilized by the adsorption of polyelectrolytes. Surfactant mono- and bilayers at interfaces are usually charged too, due to the dissociation of ionogenic chemical groups. The interaction of long oppositely charged macromolecules (polyions) with the surface can dominate the other non-electrostatic interactions and determine the grafted polyion conformation.

Being a problem of both fundamental and practical interest<sup>1</sup>, the adsorption of polyelectrolyte molecules onto oppositely charged surfaces has been studied intensively in recent years by means of analytic treatments<sup>2-6</sup>, theoretical approaches, such as numerical solutions of mean-field models<sup>7-11</sup>, and Monte Carlo simulations<sup>12-15</sup>. A number of experimental techniques like spectroscopy<sup>16</sup> and ellipsometry<sup>17</sup> has been used to measure the widths of adsorbed layers, and even the entire profiles of the adsorbed layers have been measured by means of neutron scattering techniques<sup>18,19</sup>.

However, despite these intensive investigations the full picture of polyelectrolyte adsorption on charged surfaces is still far from complete, due to the delicate interplay between chain interconnectivity and the long-range nature of the electrostatic interactions<sup>20-22</sup> as well as to the existence of several length scales<sup>6</sup>. In fact, the Monte Carlo simulations of Beltran et al.<sup>14</sup> and Kong and Muthukumar<sup>15</sup> seem to be the only studies of the conformations of isolated polyelectrolytes in the vicinity of a charged surface which provides results beyond the level of mean-field arguments.

Meanwhile, a scaling theory of conformation of a weakly charged polyelectrolyte molecule attached onto a charged surface, developed by Borisov et al.<sup>4</sup>, has proposed a number of distinct regimes of adsorption depending on the strength of electrostatic attraction to the substrate. The orientation and stretching of the grafted polyion near an oppositely charged surface are predicted to scale with the number of repeatable units (i.e. the chain length  $N$ ) of the polyion as power laws with characteristic exponents in the limit of weak screening of the Coulomb interactions.

In the present investigation we use an efficient off-lattice Monte Carlo simulational method to test these recent predictions of scaling analysis with respect to conformational and interfacial properties, and establish the critical adsorption conditions. We vary the surface and polymer charge density, the Debye-Hückel screening length, and the length of the polyion within a rather broad range ( $N \leq 512$ ) so that in result we are able to confirm the majority of the theoretical results.

## 2. The Model

We use a three-dimensional off-lattice bead-spring model<sup>23</sup> for a polyelectrolyte chain grafted with one end to an infinite plane surface, as seen in a snapshot in Fig.1.

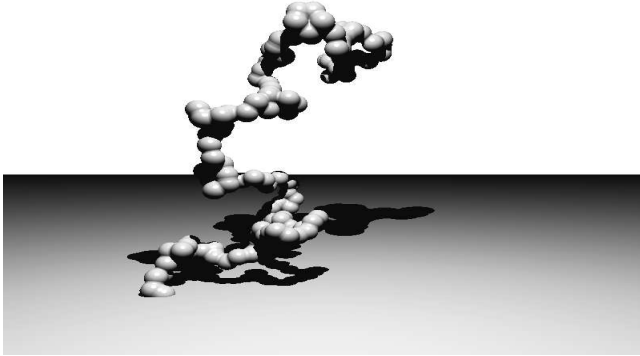


Fig. 1. Polyelectrolyte chain of length  $N = 128$  grafted to an oppositely charged surface. Linear charge density of the chain is  $q = 0.1$  elementary electrostatic units per bead. Plane charge density of the plane is  $\sigma = 0.01$  elementary electrostatic units per square unit length at the absence of salt.

The coarse-grained polymer chain consists of  $N$  beads/monomers which are successively connected by spring bonds using a finitely extensible nonlinear elastic (FENE) potential,

$$U_{FENE} = -\frac{\kappa}{2}R^2 \ln \left[ 1 - \left( \frac{l - l_0}{R} \right)^2 \right] \quad (1)$$

where  $l$  is the bond length,  $R = l_{max} - l_0$ , while  $l_0$ ,  $l_{max}$ , and  $l_{min}$  are the equilibrium value of the effective bond length, and its maximum and minimum values, respectively, such that  $l_{min} < l < l_{max}$  and  $l_{min} = 2l_0 - l_{max}$ . As in most studies using this model, we set  $l_{max} = 1$  which is taken for the elementary unit length in the simulations,  $l_{min} = 0.4$ ,  $l_0 = 0.7$ . The strength of the spring constant  $\kappa$  is fixed at  $\kappa = 40$  [ $k_B T$  units] and all simulations have been run at  $k_B T = 1$ .

The non-bonded excluded volume interactions among the beads are described by the Morse potential

$$U_M(r) = \epsilon [\exp(-2\alpha(r - r_{min})) - 2 \exp(-\alpha(r - r_{min})) + 1], \quad r < r_{min} \quad (2)$$

where  $r$  is the distance between the centers of the beads. The potential (2) is cut at its minimum point  $r_{min} = 0.8$ , and shifted upward with the value of  $\epsilon = 1$  so that at  $r_{min}$  it becomes equal to zero. This eliminates the attractive part of the Morse potential and ensures a good solvent regime for the polymer chain.

The parameter  $\alpha = 24$  is the same as in a number of previous simulations where this polymer bead-spring model has been used extensively<sup>24</sup>. With this choice of parameters of the potentials, Eq.(1) and (2), the effective radius of the bead is large enough to ensure that chains do not intersect.

The electrostatic interactions which act between two beads are described by a repulsive Debye-Hückel potential which accounts for the electrostatic screening due to the presence of salt in the solution

$$U_{DH}(r) = Aq^2 \frac{\exp(-Kr)}{r}. \quad (3)$$

The physical meaning of the parameters in Eq.(3) is as follows:  $A = l_B k_B T$  represents the dielectric properties of the medium where  $l_B = e^2 / (4\pi\epsilon k_B T)$  is the Bjerrum length (the other quantities have their usual meaning) which in our simulations is kept equal to the equilibrium bond length  $l_B = l_0 = 0.7$ .  $K^2 = l_B I$  expresses the ionic screening of the solvent, characterized by its ionic strength (salt concentration)  $I$ . We vary  $K$  from  $K \approx 1 / (Nl_{max})$  to  $K = 2.0$  so that we study all the regimes from a complete non-screening one with Debye length  $1/K \gg Nl_{max}$  down to strong

screening with  $1/K < l_0$ . Finally, the linear charge density  $q$  takes into account that not necessarily every monomer is charged. Our model distributes the charge homogeneously over the chain, such that  $q$  is the (fractional) charge on the bead ( $q = 1/m$ , where  $m$  is the number of neutral monomers between the charged beads along the chain) - at least for weakly charged polyelectrolytes this is a valid procedure<sup>25</sup>. In our simulations we varied  $q$  in the interval from  $q = 0.1$  - weakly-charged chains - to  $q = 1.6$  - strongly-charged chains.

The plane surface in our simulations is oppositely charged to the chain so that it attracts the beads of the chain with a potential that is an integral of the Debye-Hückel potential over an infinite plane. At distance  $z$  from the plane one has

$$U_S(z) = \frac{\sigma A q \exp(-Kz)}{2K}, \quad U_S(z) = \frac{-\sigma A q}{2} \left( z - \frac{Kz^2}{2} + \frac{K^2 z^3}{6} \right), \quad K < 0.001. \quad (4)$$

where  $\sigma$  is  $4\pi$  times the plane charge density of the surface and varies from  $\sigma = -10^{-5}$  to  $\sigma = -10$ . To avoid the singularity of  $U_S$  at  $K \rightarrow 0$ , we use the Taylor expansion for small  $K$  and cancel the first constant term ( $\sigma A q / 2K$ ) which gives no contribution to the attractive force between the plane and the beads.

### 3. Simulation Technique

We used the Metropolis Monte Carlo method, as described for this model in detail by Gerroff et al.<sup>23</sup>, with the following modifications:

(a) Since one of the chain ends is grafted to the plane surface, the system is localized in space and the use of periodic boundary conditions is not necessary.

(b) Because of the long-range electrostatic interactions one needs to calculate the potential energy between every pair of beads and of each bead with the plane surface. Our tests show that for a small system like a single chain of  $N \leq 512$  the fastest procedure is to calculate its energy by direct counting of all the pair energies of the beads.

(c) In order to generate uncorrelated polymer configurations we use the efficient *pivot* algorithm<sup>26</sup>. We select two beads of the chain that form a rotational axis and rotate by a random angle either the chain part between them, or the part between the free end of the chain and the nearest of the selected monomers. Instead of the slower procedure of Stellman and Gans<sup>27</sup> to correct the accumulating numeric error in off-lattice applications of the pivot algorithm we apply a number of local moves in addition to a pivot rotation. This, on one hand, keeps the chain elastic, and, on the other hand, corrects automatically the numeric errors in the pivot rotation coordinates.

However, the bond links, which are influenced by the local moves only, relax slowly to their equilibrium length, affecting eventually the estimated size of the chain as a whole. Thus one needs a fast method that can generate initial chain configurations with already equilibrated bond lengths. To this end we apply the *enhanced configurational biased*<sup>28</sup> Monte Carlo method. The chains are then constructed by taking into account that the bond lengths  $l$  between the successive beads along the chain are distributed with the proper Boltzmann probability, corresponding to the bond potential  $U_{FENE}$ . Although the configurational biased Monte Carlo method is not appropriate for the simulation of long chain molecules, it happens to be good for generating initial configurations close enough to the thermodynamic equilibrium configurations, so that the equilibration time can be decreased significantly.

Therefore our simulation procedure is as follows:

1. For each system we start with about 100 configurational biased Monte Carlo steps which generate a chain of length  $N$  with equilibrated bond lengths.
2. We use a repeated sequence of 1 pivot with 8 local move Monte Carlo steps for a certain period of time of about 1000 sequences to equilibrate the conformation of the chain without performing any measurements.
3. We continue with  $1 + 8$  sequences performing measurements after each pivot Monte Carlo step for a period of  $10^3 \div 10^4$  sequences.

With the help of this technique we were able to study strongly charged polyelectrolytes with chain lengths of up to  $N = 512$  monomers.

Such a complex simulation technique cannot be used without a proper test of its reliability and statistical correctness of the results. For  $N = 64$ , the local move Monte Carlo method is still feasible. We could therefore compare the

results for various quantities (like the bond length, the end-to-end distance, the distance of the last monomer from the surface, etc.) for both methods, and found complete agreement within statistical error bars. However, the pivot method is much more efficient: While a sweep over 25  $\sigma$  values required a total of 90 h of CPU time on an ALPHA DIGITAL AS8400/440MHz workstation for the local move method, the pivot method permitted us to obtain data of the same quality just within half an hour CPU time.

Finally we should point out that the pivot technique fails when the chain is adsorbed and lies on the surface. To avoid this problem we introduced another type of rotation around an axis passing through a random bead of the chain and perpendicular to the surface since the acceptance rate of trial 2D rotations is an order of magnitude larger than that of 3D pivot moves. Thus 2D rotation is mixed at random with 3D rotation, described above, ensuring an average acceptance rate of  $\approx 0.4$  in the pivot algorithm.

## 4. Predictions of scaling analysis

### A. Bulk behavior

Here we briefly recall the main results of the scaling theory<sup>4</sup>, describing the conformation of a weakly charged polyelectrolyte molecule attached onto a charged surface. In this theory one considers single chains immersed in a salt-free solution whereby due to the long-range character of electrostatic interactions the cooperative effects (chain orientation and additional stretching) become significant, in pronounced contrast to the case of strongly screened interactions.

In the *absence* of a charged substrate the equilibrium end-to-end distance  $H = H_0$  of a single charged macromolecule is determined by the competition between the force of intramolecular Coulomb repulsion of charged monomer units,  $f_{el}$ , and the entropic force of chain elasticity,  $f_{conf}$ :

$$f_{el} \approx k_B T \frac{N^2 q^2 l_B}{H^2}, \quad f_{conf} \approx \frac{k_B T}{l} \left( \frac{H}{Nl} \right)^{\frac{\nu}{1-\nu}}. \quad (5)$$

The balance of these two forces leads<sup>29</sup> to linear growth of the end-to-end distance  $H_0$  with  $N$ :

$$H_0 \approx Nl \left( q^2 \frac{l_B}{l} \right)^{\frac{1-\nu}{2-\nu}} \quad (6)$$

provided  $N^2 q^2 l_B \gg R_g$  where  $R_g = lN^\nu$  is the size of the coil, unperturbed by the electrostatic interactions.

In the framework of a blob picture, the polyelectrolyte molecule adopts a cigar-like form which can be presented as a succession of  $N_b$  blobs, each of size  $\xi_0 \approx k_B T / f_{el}$ , so that with  $N_b \approx N / (\xi_0 / l)^{1/\nu}$  the mean end-to-end distance (and the radius of gyration) is given by  $H_0 \approx N_b \xi_0$ , while the dimensions of the chain perpendicular to the end-to-end vector scale as  $R_\perp \approx N_b^{1/2} \xi_0$ .

### B. PreadSORption

In the presence of a weakly charged attractive plane with a force  $f_z$  acting on the polyelectrolyte chain, for  $H_0 f_z \geq k_B T$  a reorientation of the cigar-like polyion occurs whereby its conformation becomes randomly oriented in the half space above the surface, being frequently nearly parallel to the plane, so that the height  $H_z$  of the chain free end is diminished. In this regime, termed *preadsorption*, the average dimension of the chain in  $z$ -direction decreases with increasing surface charge density  $\sigma$  like

$$H_z \approx \frac{k_B T}{f_z} \approx \frac{1}{|q\sigma| l_B N}, \quad (7)$$

while the chain longitudinal dimensions remain equal to  $H_0$ . This decrease of the height,  $H_z \propto \frac{1}{\sigma}$ , continues as long as  $H_z \geq R_\perp$ .

### C. Weak compression

Upon further increase of  $\sigma$  the chain becomes laterally compressed by the electrostatic force on scales smaller than  $R_{\perp}$  but larger than  $\xi_0$ . The entropic force due to compression in  $z$ -direction is given by  $f_{conf} \approx k_B T \frac{N_b \xi_0^2}{H_z^3}$  and the balance with the compressing electrostatic force,  $f_z = -q\sigma N l_B k_B T$ , results in  $H_z \propto \sigma^{-1/3}$ . The thickness of the adsorption layer formed by the polyelectrolyte molecule at the surface is thus expected to decrease with  $\sigma$ , until  $H_z$  falls below the electrostatic blob size  $\xi_0$ , while at  $H_z \approx \xi_0$  the chain acquires a 2-dimensional conformation completely spread on the surface. In fact, the point  $H_z \approx R_{\perp}$  can be viewed as the onset of the adsorbed state, since at higher surface charge densities  $H_z$  becomes independent of  $N$ .

### D. Strong compression

Further increase in the surface charge density  $\sigma$  (and in the attraction force) deforms the electrostatic  $\xi_0$ -blobs themselves into adsorption blobs of size  $H_z$  so that the the chain part inside such a blob retains excluded volume statistics unperturbed by the electrostatic interactions. Since the charges within each blob interact with the surface with an energy  $\approx k_B T$ , the blob size (and the adsorption layer thickness) is given by  $H_z \approx l (|\sigma q| l_B l)^{-\frac{1}{1-\nu}}$ . Eventually, at still further increase of  $\sigma$ , the charges on the chain are expected to become screened by the counterions at the surface from the surface potential so that the thickness of the adsorption layer becomes independent of  $\sigma$ .

In the case of a very weakly charged chain, which in the bulk is unperturbed by Coulomb interactions, the variation of  $H_z$  with  $\sigma$  is governed by the deformation of a 3-dimensional into a 2-dimensional coil, consisting of adsorption blobs of size  $H_z$  and beginning at  $f_z R_{coil} \approx k_B T$ . According to Borisov et al.<sup>4</sup>, one observes in this case a single crossover regime with slope  $-\nu/(\nu+1)$ , spanning the two intervals of no adsorption and very strong adsorption in which  $H_z$  does not change upon variation of the surface density  $\sigma$ .

## 5. Simulational results

### A. A polyelectrolyte chain in the bulk

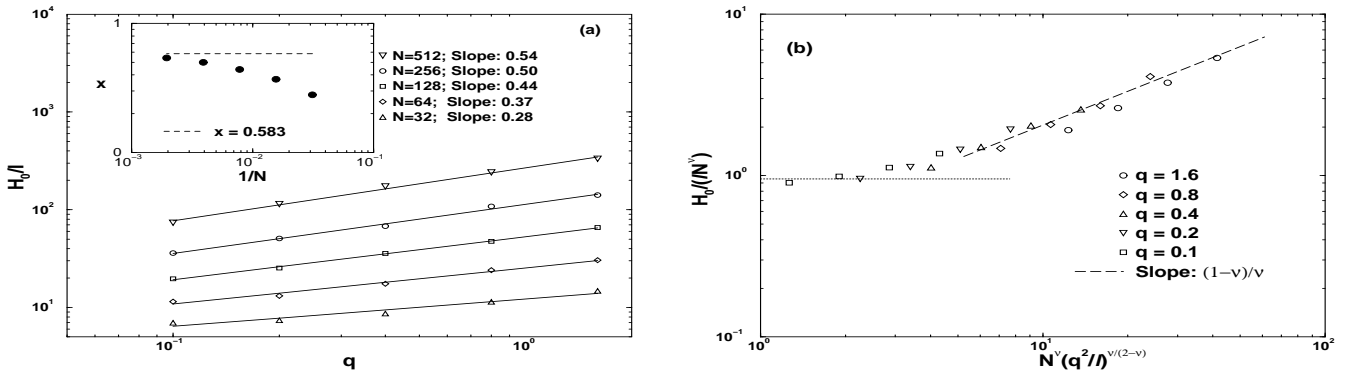


Fig. 2. (a) Scaling dependence of the dimensionless distance  $H_0/l$  on the linear charge density  $q$  for charged macromolecules of different length  $N$  in the bulk at  $K = 0$ . The variation of the measured exponent  $x$  in the power-law  $H_0/l \propto q^x$  with inverse chain length is shown in the inset. The horizontal line marks the predicted value of  $x = 2(1 - \nu)/(2 - \nu) \approx 0.583^4$ . (b) Variation of the reduced end-to-end distance  $H_0/lN^\nu$  with  $N = 32, 64, 128, 256$  with the generalized charge strength  $x = N^\nu (q^2/l)^{\nu/(2-\nu)}$ , Eq.(8) at the absence of salt, and zero surface charge density. The linear charge density  $q$  is given as a parameter. Dashed and dotted lines denote the limiting scaling behavior.

We first examine the simplest case of salt-free solution and vanishing surface charge, in which case the chain dimension should be given by Eq. 6, for sufficiently long chains. Fig. 2a presents the “raw data” for the dependence on the linear charge density  $q$ . Only for the longest chains one can observe the asymptotic  $q^{(2-2\nu)/(1-\nu)}$  behavior. In order to study also the crossover to self-avoiding walk statistics for short chains and/or weak charge, we plot in Fig. 2b the dimensionless ratio  $H_0/(lN^\nu)$ , i. e. between the chain’s actual size and its unperturbed size for zero charge. The proper scaling argument is the ratio between unperturbed chain size and electrostatic blob size, i. e.  $H_0 = lN^\nu \mathcal{F}(N^\nu (q^2 \frac{l_B}{l})^{\frac{1}{2-\nu}})$ .

From the requirement  $H_0 \propto lN^\nu$  for  $q \rightarrow 0$ , and  $H_0 \propto lN$  for large  $q$  one gets for  $\mathcal{F}(\zeta)$ :

$$\mathcal{F}(\zeta) \propto \begin{cases} \text{const.} & \zeta \rightarrow 0, \\ \zeta^{\frac{1}{\nu}-1} & \zeta \gg 1; \end{cases} \quad (8)$$

this behavior is indeed observed (some scatter in the data is presumably due to corrections to scaling which are important for the shorter chain lengths,  $N = 32, 64$ ). It should be noted that the measured values of  $H_0$  are divided here by the actually measured bond length  $l$  in order to take into account its systematic increase with  $q$ , amounting to up to 10% for the strongest charge.

## B. A polyelectrolyte chain near an oppositely charged surface

In Fig. 3 we show the measured variation of  $H_z$ , the chain free end distance from the charged plane, with  $\sigma$ , the surface density, which is here varied over more than five orders of magnitude, for different values of the screening parameter  $K$ . Evidently, all data for  $K \rightarrow 0$  saturate to a single curve that corresponds to the unscreened Coulomb interaction regime,  $K = 0$ . In this regime the data confirm rather well the expected behavior in the regimes of preadsorption, Sec. 4B, and strong compression, Sec. 4D. For a strongly charged chain with  $N = 256$ , (Fig. 3a), at  $K \rightarrow 0$ , the sampled  $H_z$  vs.  $\sigma$  relationship matches closely the slopes of  $-1$  (“preadsorption”), and of  $-\nu/(\nu+1) \approx -0.37$  (“strong compression”), considered in Section 4. The only regime which is not observed here is the intermediate slope of  $-1/3$  in between these two regimes. This transitional regime, if existent, is masked by the curvature of the crossover region. The proximity of its exponent ( $-0.33$ ) to that of the strongly adsorbed macromolecule ( $-0.37$ ) gives little hope that it can be unambiguously established. One also cannot rule out a possible “finite size” effect due to insufficient chain length, although with  $N = 256$  the other regimes are observed clearly. For a weakly charged chain, it is evident from Fig.3b that at  $K \rightarrow 0$  the expected behavior  $H_z \propto \sigma^{-\frac{\nu}{\nu+1}}$  is very well established. As the screening parameter  $K$  grows, the transition from the non-adsorbed to the adsorbed state becomes steeper, Fig. 3.

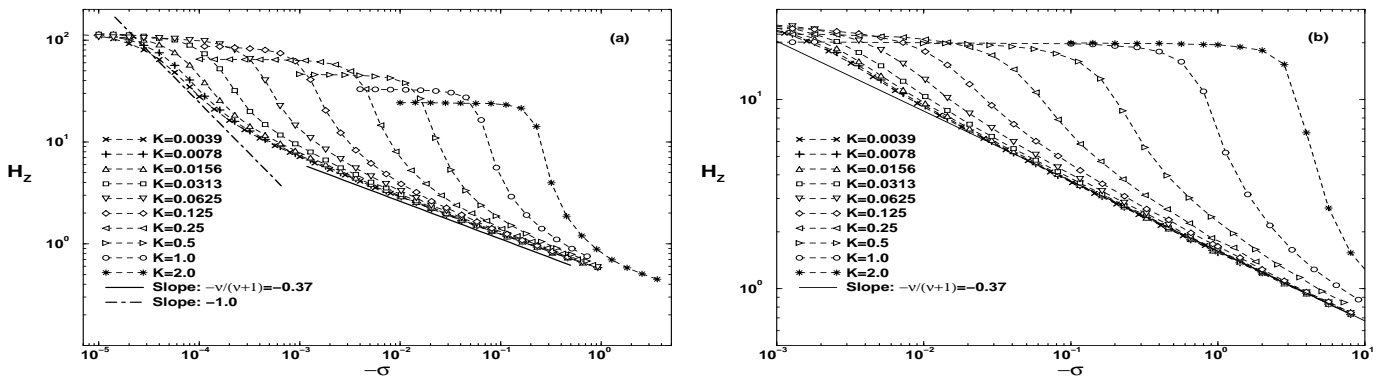


Fig. 3. Distance  $H_z$  of the free end of a chain of  $N = 256$  from the plane surface vs. surface charge density  $\sigma$  for a set of  $K$  values. (a) Strongly charged chain ( $q = 1.6$ ) and (b) weakly charged chain ( $q = 0.1$ ). Straight lines denote the expected scaling behavior<sup>4</sup> at  $K = 0$ .

It is instructive to take a closer look at the case of completely unscreened electrostatic interactions,  $K = 0$ , using the relative height  $H_z/R_g$  of the chain, where  $R_g$  is the gyration radius. In the preadsorption regime, Eq. 7 states

that  $H_z \propto 1/(|\sigma|N)$ , while  $R_g \propto N$  so that  $H_z/R_g \propto (|\sigma|N^2)^{-1}$ . Thus one may expect that the plot of  $H_z/R_g$  vs.  $|\sigma|N^2$  should give a region where the data for chains of equal charge density  $q$ , but different chain lengths  $N$  should lie on a single master curve, which would mark the preadsorption regime. The data for the shorter chains with a smaller preadsorption region would leave the curve sooner on the right and left side, while the larger chain data would keep staying on the preadsorption curve longer. This behavior is indeed observed in Fig. 4a for  $q = 1.6$  and 0.4. To be consistent with the transition plots of Fig. 6 and because of the fact that the measured quantities are  $\langle H_z^2 \rangle$  and  $\langle R_g^2 \rangle$  we have plotted in a semi-log plot the ratio  $H_z^2/R_g^2$  vs.  $|\sigma|N^2$  (but not vs.  $(|\sigma|N^2)^2$ , because the log-scale of the x-axis only turns the squaring of  $(|\sigma|N^2)$  into a prefactor of two). However, for weakly charged chains ( $q = 0.1$ ) no master curve is found, which is well understood by remembering that sufficiently weakly charged chains do not exhibit a preadsorption regime (see Sec. 4D and Fig. 3b). In that case, one only has the strong compression regime, in which the electrostatic blob size is identical with  $H_z \propto |\sigma|^{-\nu/(1+\nu)}$ . Building up the adsorbed chain from the blobs, one finds a scaling argument  $N|\sigma|^{1/(1+\nu)}$  or  $|\sigma|N^{1+\nu}$ , verified in the inset of Fig. 4a.

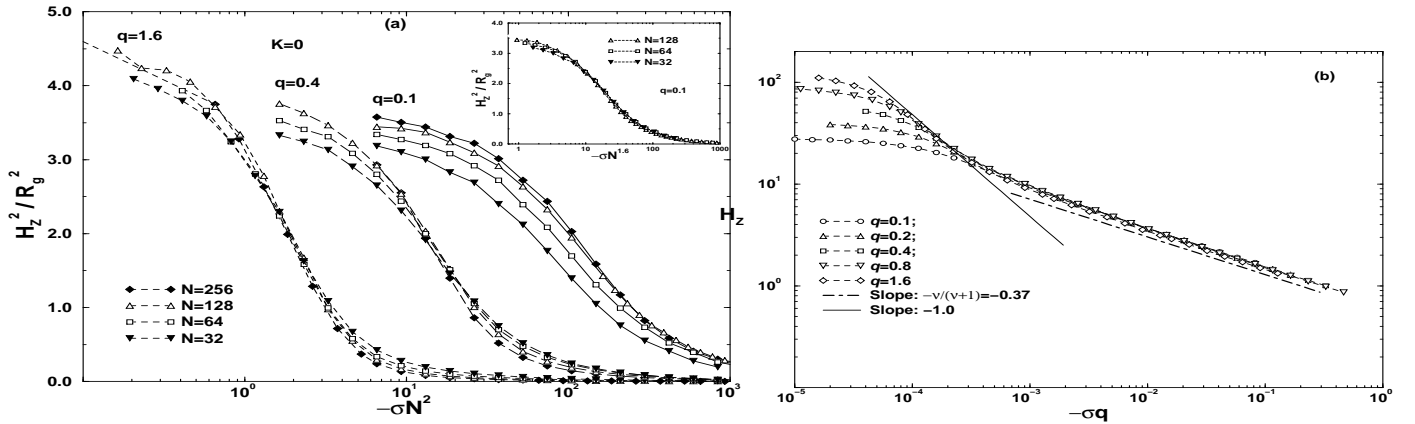


Fig. 4. (a) Variation of the ratio  $H_z^2/R_g^2$  with  $\sigma N^2$  for three different linear charge densities of the polyon,  $q = 0.1, 0.4, 1.6$ . The inset gives the ratio  $H_z^2/R_g^2$  for  $q = 0.1$  vs.  $\sigma N^{1+\nu}$ . (b) Variation of  $H_z$  with  $\sigma q$  of a polyelectrolyte chain with  $N = 256$  monomers. Both plots are at  $K = 0$ .

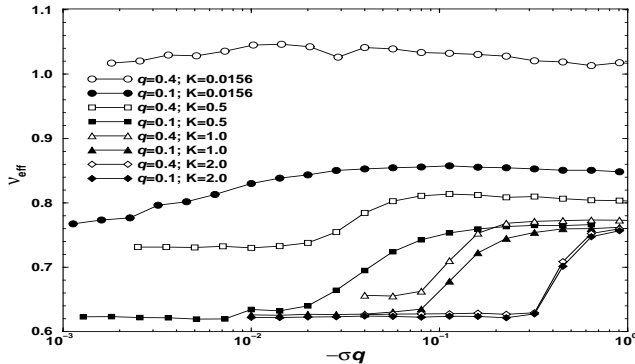


Fig. 5. Variation of the effective Flory exponent  $\nu_{eff}$  with surface charge density  $\sigma$  for different values of linear charge density  $q$  and screening parameter  $K$ , given in the figure.

The progressive growing of the preadsorption regime with the gradual increase of the charge strength of the chain is demonstrated by Fig. 4b. An increase in the linear charge density  $q$  results in a decrease of the electrostatic blob size, as discussed by Borisov et al.<sup>4</sup>, which in turn increases the number of blobs and is manifested by the formation of a well-established preadsorption regime.

The crossover of the state of the charged coil from a nonadsorbed into a strongly adsorbed one can also be

characterized by an effective exponent  $\nu_{eff}$ , describing how the chain gyration radius  $R_g$  scales with chain length  $N$ ,  $R_g \propto N^{\nu_{eff}}$ . This is illustrated in Fig. 5 where one can see that for large  $K = 2.0, 1.0$ , there is a clear transition from 3-dimensional behavior with  $\nu_{eff} = 0.62 \div 0.65$  (a value slightly larger than  $\nu_{3d} = 0.588$  due to the existence of chain charge  $q \neq 0$ ) of a desorbed chain to  $\nu_{eff} = 0.76 \div 0.78$  in the adsorbed regime, characterized by  $\nu_{2d} = 3/4$ . If the electrostatic interactions become progressively unscreened by decreasing  $K$  (and thus increasing the Debye length), this crossover is gradually leveled off and practically disappears at  $K = 0.0156$ ,  $q = 0.4$ . In the latter regime of nearly pure Coulomb interaction the chain is stretched in both desorbed and adsorbed state, and therefore no change in the exponent  $\nu_{eff} \approx 1$  is observed.

### C. The adsorption transition

As long as the Debye screening parameter  $K$  is finite, the chain will asymptotically (i. e. for sufficiently long chain length  $N$ ) behave like a neutral chain, i. e. it will obey self-avoiding walk statistics in the absence of the attractive surface. Since, for  $K > 0$ , the attraction potential is also short-ranged, one has just the well-known case of adsorption with short-ranged attractive interactions<sup>30</sup>. The adsorption transition then becomes a sharp second-order thermodynamic phase transition which occurs at a well-defined value  $\sigma = \sigma_c$  (note that increasing the surface attraction is equivalent to lowering the temperature, in terms of which the transition is usually discussed). Of course, a sharp transition is only possible in the thermodynamic limit  $N \rightarrow \infty$ , i. e.  $\sigma_c$  cannot depend on chain length.

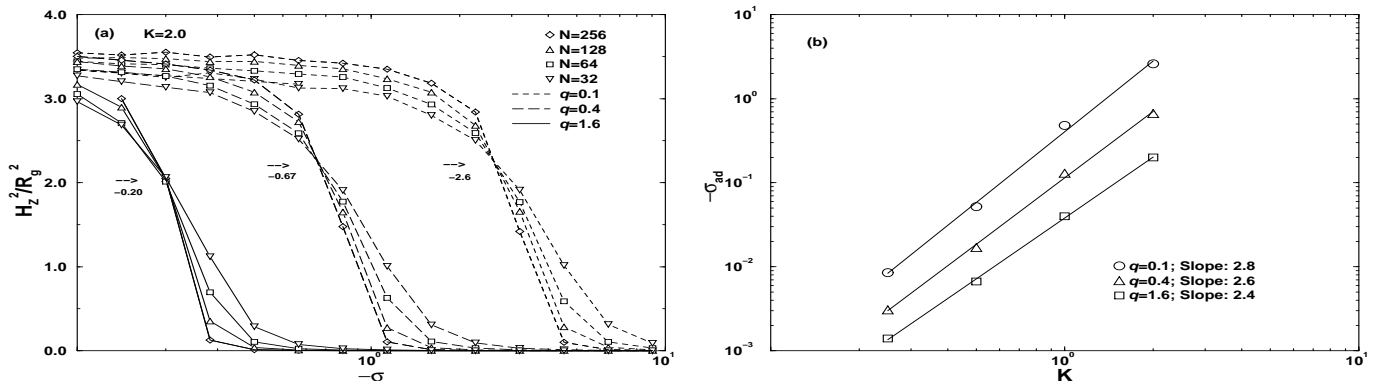


Fig. 6. (a) Variation of the ratio  $H_z^2/R_g^2$  with surface charge density  $\sigma$  for polyions of length  $N = 32, 64, 128, 256$  and  $K = 2.0$ . The resulting values of  $\sigma_c$  for three different linear charge densities,  $q = 0.1, 0.4, 1.6$  are marked by arrows. (b) Log-log plot of  $\sigma_c$  vs.  $K$  for three values of the linear charge density  $q$ .

In order to determine the asymptotic sharp value  $\sigma_c$ , we employ finite-size scaling by studying the variation of the ratio  $H_z^2/R_g^2$  (which can be viewed as a critical amplitude ratio) with  $\sigma$ . For desorbed chains,  $|\sigma| < |\sigma_c|$ , one would expect that  $H_z/R_g = const.$  in the thermodynamic limit. However, for finite chains the ratio will slightly grow upon decreasing  $|\sigma|$ , as the polymer “mushrooms” get deformed due to entropic repulsion from the wall. On the other hand, in the adsorbed state  $H_z$  should be independent of chain length  $N$ , such that the ratio  $H_z^2/R_g^2 \rightarrow 0$  when  $N \rightarrow \infty$ . This decrease of the ratio becomes sharper and sharper when  $N$  is increased. For  $\sigma = \sigma_c$  the curves corresponding to different chain lengths  $N$  should intersect in a single point which is identified as the critical point at which the adsorption occurs. And indeed, by varying  $\sigma$  over three orders of magnitude - Fig. 6a - this expected behavior of  $H_z^2/R_g^2$  can clearly be demonstrated for various large values of the inverse Debye screening length  $K = 2.0, 1.0, 0.5, 0.25$ . From Fig. 6a it is thus evident that the critical surface charge density  $\sigma_c$  may be reliably determined as long as  $K$  is sufficiently large.

For larger screening lengths, one needs longer and longer chains in order to observe the correct asymptotic chain statistics. Nevertheless, also in this case one will ultimately have a well-defined adsorption transition at a finite value  $\sigma_c$  independent of chain length, although, due to our limitations in computer resources, we were not able to resolve it reliably for  $K$  smaller than 0.25. Since an infinite Coulomb chain is *always* adsorbed, one obviously must have  $\sigma_c \rightarrow 0$  for  $K \rightarrow 0$ . This behavior is studied in Fig. 6b in a log-log representation. We find a power law whose

effective exponent gradually decreases with charge density  $q$ , i. e.  $|\sigma_c| \propto K^{2.8}$  for  $q = 0.1$  while  $|\sigma_c| \propto K^{2.4}$  for  $q = 1.6$ . It should be noted that this  $K$  dependence is similar to the exponents predicted by Muthukumar et al.<sup>3,15</sup> ( $K^3$  and  $K^{11/5}$  in various regimes). However, this analytical study also predicts a chain length dependence of the critical adsorption parameter. In our opinion, this is a contradiction in itself, since the condition of criticality can only be *defined* in the thermodynamic limit, which we try to reach by our finite-size scaling procedure.

#### D. Adsorbed layer thickness

Finally we consider an important quantity of practical interest - the width of the adsorbed polyelectrolyte layer. In Fig. 7a we show the measured thickness of the adsorbed layer and examine its dependence on  $\sigma$  and  $K$ . If the chain is adsorbed, the free end distance  $H_z$  from the substrate should not depend on the chain length  $N$ . We here define the thickness of the adsorbed layer as the limiting value of  $H_z$  (if it exists) with growing chain length  $N$ . The plus signs on the vertical dashed lines on Fig. 7a mark these  $H_z$  values for several values of  $\sigma$ . Indeed, in nearly all cases the data for different chain length  $N$  collapse on a single point (plus symbol), demonstrating that an asymptotic value has been found. The only questionable point is the upper-most plus sign at  $\sigma = -3.2$  concerning the data at  $K = 2.0$ . But from Fig.6a one can verify that for  $K = 2.0$  we obtain  $\sigma_c = -2.6$  which is a weaker charge than  $-3.2$  so that a long enough chain with  $N > 512$  should have probably been used in the simulation in order to reach proper adsorption. Unfortunately, such chain lengths are still beyond our possibilities in terms of computational effort so we assume the value  $H_z$  of  $N = 512$  to be the closest estimate for the layer thickness at  $\sigma = -3.2$  and  $K = 2.0$ .

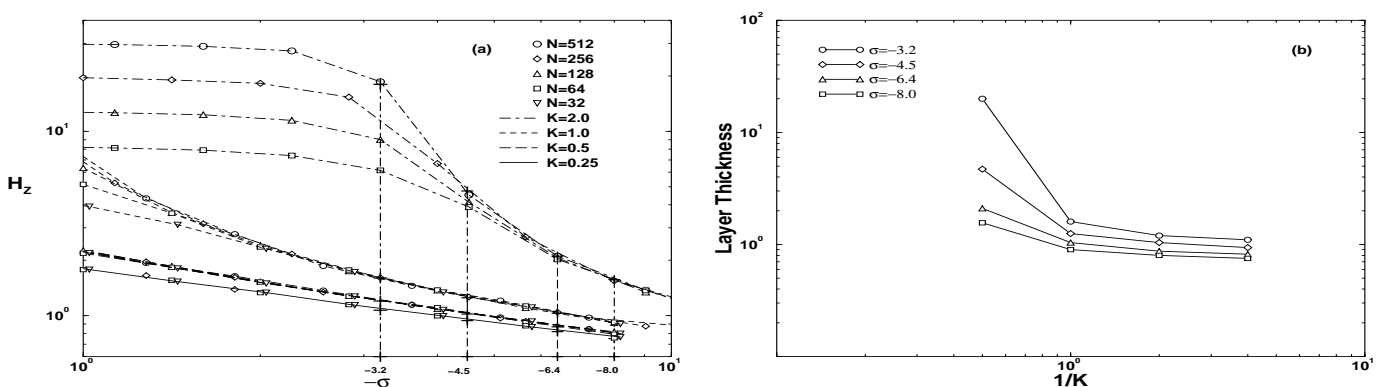


Fig. 7. (a) Variation of the polymer end distance  $H_z$  from the charged plane with surface charge density  $\sigma$  for chain lengths  $N = 32, 64, 128, 256, 512$  and  $K = 0.25, 0.5, 1.0, 2.0$  for  $q = 0.1$ . (b) Variation of the measured layer thickness with the Debye screening length  $K^{-1}$  at four surface charge densities  $\sigma$ , given as a parameter.

In Fig. 7b we plot the dependence of the layer thickness, measured from Fig. 7a, on the Debye screening length  $K^{-1}$ . Evidently, for  $K \leq 1$  this dependence is qualitatively in good agreement with the self-consistent field numerical calculations of Varoqui<sup>8</sup> and with the recent simulational results<sup>15</sup> although our data do not comply with the prediction by Muthukumar<sup>3</sup> that the adsorption layer thickness should be proportional to  $K^{-1}$ .

#### 6. Conclusions

Polyelectrolytes are fascinating materials that can be studied with the use of Monte Carlo simulations. We have shown that a continuous model with rather simple potentials allows us to study in detail polyelectrolyte adsorption and verify some recent theoretical predictions.

In particular, we have shown that the scaling approach of Borisov et al.<sup>4</sup> provides a faithful description of the interaction of polymers chains with charged surfaces at small length scales. The simulational results reproduce the scaling configurational properties of adsorbed polyions remarkably well.

We also suggest a finite-size scaling method for the determination of the critical surface charge density at which

the adsorption of the polyion takes place. With it we find a power law variation of the critical surface density with the Debye screening length which is within the range of values for the exponent predicted earlier by Muthukumar<sup>3</sup>.

However, despite of these new results a lot of work is still needed until the complex problem of polyelectrolyte adsorption for screened Debye-Hückel chains (not even considering the richer physics which comes in from the counterion degrees of freedom, like, e. g. Manning condensation) is fully understood. A scaling function, describing faithfully the adsorption transition in terms of the polyion chain length, the Debye screening length, the electrostatic blob size, and the surface charge density, can only be constructed if there is a good understanding of the variation of the persistence length with the Debye length. This problem is complicated and a target of further research.

## 7. Acknowledgments

Acknowledgment is made to the Volkswagen Foundation (Grant No. I/72 164) for support of this research.

- 
1. D. H. Napper, *Polymeric Stabilization of Colloid Dispersion*, Colloid Science, Academic Press, New York, 1983.
  2. F. W. Wiegel, *J. Phys. A: Math. Gen.* **10**, 299 (1976).
  3. M. Muthukumar, *J. Chem. Phys.*, **86**, 7230 (1987).
  4. O. V. Borisov, E. B. Zhulina and T. M. Birshtein, *J. Phys. II France* **4**, 913 (1994).
  5. X. Chatellier and J. F. Joanny, *J. Phys. II France* **6**, 1669 (1996).
  6. I. Boruchov, D. Andelman, and H. Orland, *Macromolecules* **31**, 1665 (1998).
  7. O. A. Evers, G. J. Fleer, J. M. Scheutjens, and J. J. Lyklema, *J. Colloid Interface Sci.* **111**, 446 (1986).
  8. R. Varoqui, *J. Phys. II France* **3**, 1097 (1993).
  9. I. Boruchov, D. Andelman, and H. Orland, *Europhys. Lett.* **32**, 499 (1995).
  10. P. Linse, *Macromolecules* **29**, 326 (1996).
  11. V. Shubin and P. Linse, *Macromolecules* **30**, 5944 (1998).
  12. T. Akeson, C. Woodward, and B. Jönsson, *J. Chem. Phys.* **91**, 2461 (1989).
  13. T. Wallin and P. Linse, *Langmuir* **12**, 305 (1996).
  14. S. Beltran, H. H. Hooper, H. W. Blanch, and J. M. Prausnitz, *Macromolecules* **24**, 3178 (1991).
  15. C. Y. Kong and M. Muthukumar, *J. Chem. Phys.* **109**, 1522 (1998).
  16. J. Meadows, P. A. Williams, M. J. Garvey, R. Harrop, and G. O. Phillips, *J. Colloid Interface Sci* **132**, 319 (1989).
  17. V. Shubin, and P. Linse, *J. Phys. Chem.* **99**, 1285 (1995).
  18. P. Auroy, L. Auvray, and L. Leger, *Macromolecules* **24**, 2523 (1991).
  19. O. Guislein, L. T. Lee, B. Farnoux, and A. Lapp, *J. Chem. Phys.* **95**, 4632 (1991).
  20. F. Oosawa, *Polyelectrolytes*, Marcel Dekker, New York, 1971.
  21. T. Odijk, *Macromolecules* **12**, 688 (1979).
  22. A. V. Dobrynin, R. H. Colby, and M. Rubinstein, *Macromolecules* **28**, 1859 (1995).
  23. I. Gerroff, A. Milchev, W. Paul, and K. Binder, *J. Chem. Phys.* **98**, 6526 (1993).
  24. For an overview see A. Milchev, *Conformational and Dynamic Properties of Polymer Chains, Adsorbed on Hard Surfaces*, in *Computational Methods in Colloid and Interface Science*, Ed. M. Borowko, Marcel Dekker, New York, 1999, Ch. 9 (in press).
  25. A. Lyulin, B. Dünweg, O. Borisov and A. Darinskii, *Macromolecules*, in press.
  26. N. Madras and A. D. Sokal, *J. Stat. Phys.* **50**, 109 (1988).
  27. S. D. Stellman and P. J. Gans, *Macromolecules* **5**, 516 (1972).
  28. D. Frenkel and B. Smit, *Understanding Molecular Simulation: From Algorithms to Application*, Academic Press, NY (1996) pp. 292-300.
  29. P. G. de Gennes, P. Pincus, R. M. Velasco, and F. Brochard, *J. Physique* **37**, 1461 (1976).
  30. E. Eisenriegler, *Polymers Near Surfaces*, World Scientific, Singapore, 1993